

**Supplemental material:****Intratumoral combination therapy with poly(I:C) and resiquimod synergistically triggers tumor-associated macrophages for effective systemic antitumoral immunity****Authors:**

Clément Anfray<sup>1</sup>, Francesco Mainini<sup>1</sup>, Elisabeth Digifco<sup>1,2</sup>, Akihiro Maeda<sup>1</sup>, Marina Sironi<sup>1</sup>, Marco Erreni<sup>1</sup>, Achille Anselmo<sup>1</sup>, Aldo Ummarino<sup>1,2</sup>, Sara Gandoy<sup>3</sup>, Francisco Expósito<sup>4</sup>, Mirian Redrado<sup>4</sup>, Diego Serrano<sup>4</sup>, Alfonso Calvo<sup>4</sup>, Marvin Martens<sup>5</sup>, Susana Bravo<sup>6</sup>, Alberto Mantovani<sup>1,2</sup>, Paola Allavena<sup>1,2</sup> and Fernando Torres Andón<sup>1,3</sup>

**Affiliations:**

<sup>1</sup>IRCCS Istituto Clinico Humanitas, Rozzano, Italy

<sup>2</sup>Humanitas University, Pieve Emanuele, Italy

<sup>3</sup>Center for Research in Molecular Medicine and Chronic Diseases, Santiago de Compostela, Spain

<sup>4</sup>Department of Pathology, Anatomy and Physiology, University of Navarra, Pamplona, Spain

<sup>5</sup>Department of Bioinformatics, Maastricht University, Maastricht, Netherlands

<sup>6</sup>Health Research Institute of Santiago de Compostela, Santiago de Compostela, Spain

**This PDF file includes:**

Supplementary Methods

Supplementary Table 1-8

Supplementary Figures 1-11

## Supplementary methods

### Toxicity assay on CMT167 cells *in vitro*

CMT167 cancer cells ( $10^4$  cells/well) were cultured in 96 well black microplates (Corning) and treated with the indicated concentrations of drugs in appropriate cell culture medium. After indicated times, cell viability was assessed with the Alamar Blue Assay (Invitrogen) following manufacturer's protocol. Fluorescence intensity was measured with a Synergy H4 plate reader (BioTek), setting the  $\lambda_{\text{abs}}$  at 544 nm and the  $\lambda_{\text{em}}$  at 590 nm. Non-treated cells were used as controls and considered as 100% cell viability. The following equation was used to calculate the cell viability:

$$\text{Cell viability (\%)} = (1 - \text{fluorescence/control fluorescence}) * 100.$$

**Culture of bone marrow derived murine macrophages.** Bone-marrow derived murine macrophages (BMDMs) were obtained from femurs and tibias of healthy C57Bl/6 mice (Charles River). Briefly, bones were collected and washed in PBS (Sigma-Aldrich). The bone marrow was flushed with 1 ml 5% FBS RPMI using a 21G needle. The bone marrow was then homogenized by pipetting up and down several times, then passed through a  $0.7 \mu\text{m}$  filter to obtain a cell suspension. After centrifugation cells were suspended 5 min in ACK lysis buffer to eliminate red blood cells. Cells were washed in PBS then suspended in 5% FBS RPMI supplemented with murine M-CSF (PeproTech) at a concentration of 25 ng/ml and plated at a density of  $10^6$  cells/ml.

**Measurement of cytokine secretion and NO.** Cytokine secretion and NO production was measured by commercially available ELISA kits (murine CXCL10 and TNF- $\alpha$ , R&D Systems) and the Griess Reagent System (Promega), respectively, according to manufacturer's instructions (R&D Systems), using the supernatants collected 24 h after each indicated treatment.

**Cytotoxic activity of murine BMDMs towards murine CMT167 cells.** CMT167 cells, suspended in PBS, were stained with CellTrace™ Far Red 1 mM (Invitrogen) for 20 min at room temperature, then washed with complete RPMI. In 24 well plates (Corning),  $2 \times 10^4$  of these stained CMT167 cells were co-cultured with  $10^6$  murine BMDMs, previously exposed to TLRs agonists for 24 h, in fresh 5% FBS RPMI. After 2 days, cells were harvested and fixed for flow cytometry analysis using a FACS Canto II instrument (BD

Biosciences). For flow cytometry analysis, high fluorescent intensity events, corresponding to CMT167 cells, were counted, for 45 seconds of acquisition time. The values were normalized to the non-treated M0 macrophages.

**Multiplexed analysis of circulating cytokines.** Plasma samples were obtained at the end of the experiment. Levels of IL-6 and TNF- $\alpha$  were quantified in a customized multiplexed format with a murine-specific MILLIPLEX MAP kit (Merck-Millipore) according to the manufacturer's instructions and run on a Luminex MAGPIX system (Merck-Millipore).

**Immunohistochemistry for CD11c.** For immunohistochemistry, sections were hydrated and endogenous peroxidase was blocked with a 3% hydrogen peroxide solution. Antigen retrieval was done with Citrate buffer (pH= 6, 20 min at 98°C). After incubation with normal goat serum to block unspecific binding, anti-CD11c (1:50, D1V9Y Rabbit mAb #97585 Signaling) and the Envision system (Dako, Denmark), followed by DAB (3,3'-diaminobenzidine; Dako) and counterstaining with haematoxylin were applied prior to observation. IHC images were first scanned with the Aperio CS2 (Leica) scanner at 20x magnification. Images were visualized with the Image Scope (v12.1.05029, from Aperio, Leica) software. Image analysis was performed using Qupath (Bankhead, P. et al. QuPath: Open source software for digital pathology image analysis. *Scientific Reports* (2017). <https://doi.org/10.1038/s41598-017-17204-5>). Briefly, tumor tissue ROIs were manually selected to exclude necrotic areas and images were thresholded to generate the CD11c positive areas classifier. Quantification was performed using the ration CD11c/total tumor area per image.

**Supplementary Table 1.** List of antibodies used for multiplexed tumor immunophenotyping.

Antibodies (Ref)	Dilution	Antigen retrieval	Opal/Dilution
CK (CST,4279)	1:100	TrisEDTA buffer, pH9	690/1:100
CD31 (CST, 77699)	1:400	Citrate buffer, pH6	570/1:600
F4/80 (CST, 70076)	1:400	Citrate buffer, pH6	650/1:600
CD8 (Thermo, C8/14bb)	1:400	PerkinElmer reagent, pH6	570
CD4 (Dako, 4B12)	Ready to use	Dako reagent, pH9	650
Foxp3 (PE, OP7TL1001KT)	1:300	PerkinElmer reagent, pH6	620
iNos (CST, 13120)	1:400	Citrate buffer, pH6	650/1:50
Arg1 (CST, 93668)	1:100	Citrate buffer, pH6	570/1:50
F4/80 (CST, 70076)	1:400	Citrate buffer, pH6	520/1:50

**Supplementary Table 2.** List of antibodies and primers used for flow cytometry and RT-PCR.

Antibodies	Reference	Dilution
CD45-PerCP	557235; Clone 30-F11 (BD Biosciences)	1:200
Cd11b-APC eFluor780	47-0112-82; Clone M1/70 (eBiosciences)	1:400
CD11c-APC	550261; Clone HL3 (BD Biosciences)	1:100
Ly-6G-PE-Cy7	552877; Clone 53-6.7 (BD Biosciences)	1:250
F4/80-PE	MCA497PE; Clone Cl:A3-1 (BioRad)	1:50
MHCII-Alexa488	107616; Clone M5/114.15.2 (BioLegend)	1:500
CD206-BV421	141717; Clone C068C2 (BioLegend)	1:500
NK1.1-PE	12-5941-82; Clone PK136 (eBiosciences)	1:100
CD3e-APC	17-0031-82; Clone 145-2C11 (eBiosciences)	1:125
CD4-FITC	100510; Clone RM4-5 (BioLegend)	1:150
CD8a-PE-Cy7	552877; Clone 53-6.7 (BD Biosciences)	1:500
CD69-PE-CF594	562455; H1.2F3 (BD Biosciences)	1:100
PD1-PE	109104; Clone RMP1-30 (BioLegend)	1:50
CD44-FITC	561859; Clone IM7 (BD Biosciences)	1:250
CD62L-APC	553152; Clone MEL-14 (BD Biosciences)	1:250
Primers	Sequence 5' – 3'	
GADPH for	AACGACCCCTTCATTGAC	

GADPH rev	TCCACGACATACTCAGCAC
IRF7 for	AAACCATAGAGGCACCCAAG
IRF7 rev	CCCAATAGCCAGTCTCCAAA
INF- $\gamma$ for	ATGAACGCTACACACTGCATC
INF- $\gamma$ rev	CCATCCTTTTGCCAGTTCCTC
CCL5 for	TACCATGAAGATCTCTGCAGCT
CCL5 rev	CTGCTGGTGTAGAAATACTCCT
CXCL10 for	GACGGTCCGCTGCAACTG
CXCL10 rev	CTTCCCTATGGCCCTCATTCT
iNOS for	CGAAACGCTTCACTTCCAA
iNOS rev	TGAGCCTATATTGCTGTGGCT
Granzyme B for	CCACTCTCGACCCTACATGG
Granzyme B rev	GGCCCCCAAAGTGACATTTATT
Perforin for	AGCACAAAGTTCGTGCCAGG
Perforin rev	GCGTCTCTCATTAGGGAGTTTTT

**Supplementary Table 3.** Number of identified proteins significantly changed by each treatment in the quantitative proteomic analysis (p-value  $\leq$  0.05).

SWATH-MS	Upregulated (vs. control)	Downregulated (vs. control)	Total (vs. control)
poly(I:C)	42	46	88
R837	90	30	120
R848	41	26	67
poly(I:C) + R837	86	31	117
Poly(I:C) + R848	113	52	165

**Supplementary Table 4.** Number of proteins measured for each GO-term in the quantitative proteomic analysis (p-value  $\leq$  0.05).

GO-term ID	GO-term title	Proteins in the GO-term	Measured proteins in the GO-term
GO:0006955	immune response	1500	94
GO:0045087	innate immune response	810	66
GO:0002250	adaptive immune response	489	25
GO:0001906	cell killing response to cytokine	83	14
GO:0034097	Response to cytokine	766	83
GO:0006979	Response to oxidative stress	342	45
GO:0006915	apoptotic process	809	63

**Supplementary Table 5.** Number of proteins identified in treated tumors.

LC-MS	Proteins Identified
Control	1039
poly(I:C)	1064
R837	1046
R848	1188
poly(I:C) + R837	955
poly(I:C) + R848	1123

**Supplementary Table 6.** Number of proteins measured for each biological process in the qualitative proteomic analysis using FunRich (<http://www.funrich.org/>).

Biological process	Total number of proteins in the process	Number of proteins measured for each treatment in the biological process					
		Control	poly(I:C)	R837	R848	poly(I:C) + R837	poly(I:C) + R848
immune response	345	7	11	8	8	8	13
innate immune response	600	36	44	40	39	45	42
adaptive immune response	315	13	15	13	12	12	17
Positive regulation of T cell mediated cytotoxicity	56	4	7	5	4	7	7
Positive regulation of cytokine secretion	67	4	4	4	2	4	5
Cellular response to oxidative stress	132	9	9	9	2	9	8
Apoptotic process	705	33	37	38	34	39	27
Positive regulation of T cell migration	29	1	1	1	2	1	2

**Supplementary Table 7.** List of the up-regulated proteins in poly(I:C)+R848 treated tumors. FC, Fold change.

Up-regulated					
Protein	UniProt ID	UniProt accession	p-value	FC	Log 2 (FC)
Alpha-1-acid glycoprotein 2	A1AG2_MOUSE	P07361	0.020807	9.392404	3.231494
Translationally-controlled tumor protein	TCTP_MOUSE	P63028	0.001436	5.897405	2.56008
Serine protease inhibitor A3N	SPA3N_MOUSE	Q91WP6	0.04331	5.4535	2.447182
Myristoylated alanine-rich C-kinase substrate	MARCS_MOUSE	P26645	0.011078	5.43516	2.442323
Haptoglobin	HPT_MOUSE	Q61646	0.002553	5.364626	2.423478
Interferon-induced protein with tetratricopeptide repeats 2	IFIT2_MOUSE	Q64112	0.043334	4.786776	2.259054
E3 ubiquitin-protein ligase TRIP12	TRIPC_MOUSE	G5E870	0.001927	4.444574	2.152045
Reticulocalbin-1	RCN1_MOUSE	Q05186	0.025571	4.382208	2.131658
Osteopontin	OSTP_MOUSE	P10923	0.007896	4.199009	2.070049
Peptidyl-prolyl cis-trans isomerase FKBP3	FKBP3_MOUSE	Q62446	0.011224	4.17302	2.061092
Neutrophilic granule protein	NGP_MOUSE	O08692	0.002169	4.119315	2.042404
Tropomyosin alpha-1 chain	TPM1_MOUSE	P58771	0.027483	3.991526	1.99694
Proteasome adapter and scaffold protein ECM29	ECM29_MOUSE	Q6PDI5	0.039021	3.984314	1.994331
Interferon-induced protein with tetratricopeptide repeats 3	IFIT3_MOUSE	Q64345	0.011041	3.511872	1.81224
Interferon-activable protein 205-B	IFI5B_MOUSE	P0DOV1	0.008885	3.436932	1.781121
Rho GDP-dissociation inhibitor 2	GDIR2_MOUSE	Q61599	0.016532	3.411876	1.770565
Exportin-5	XPO5_MOUSE	Q924C1	0.043807	3.165957	1.662641
Interferon-inducible GTPase 1	IIGP1_MOUSE	Q9QZ85	0.003423	3.164299	1.661886
Parathyrosin	PTMS_MOUSE	Q9D0J8	0.026193	3.109102	1.636498
Myosin regulatory light chain 12B	ML12B_MOUSE	Q3THE2	0.037891	3.012188	1.590812
V-type proton ATPase subunit E 1	VATE1_MOUSE	P50518	0.03945	2.998174	1.584084
E3 ubiquitin-protein ligase HUWE1	HUWE1_MOUSE	Q7TMY8	0.0357	2.963595	1.567348
Zinc-alpha-2-glycoprotein	ZA2G_MOUSE	Q64726	0.011613	2.891377	1.531757
Signal transducer and activator of transcription 1	STAT1_MOUSE	P42225	0.001746	2.851739	1.511842
Barrier-to-autointegration factor	BAF_MOUSE	O54962	0.020133	2.794917	1.482805
Isoamyl acetate-hydrolyzing esterase 1 homolog	IAH1_MOUSE	Q9DB29	0.034122	2.794759	1.482724
Ubiquitin-like protein ISG15	ISG15_MOUSE	Q64339	0.008337	2.742875	1.455689
Septin-7	SEPT7_MOUSE	O55131	0.010371	2.735326	1.451713
Y-box-binding protein 3	YBOX3_MOUSE	Q9JKB3	0.013025	2.704532	1.435379
Endoplasmic reticulum resident protein 44	ERP44_MOUSE	Q9D1Q6	0.019793	2.69248	1.428936
H-2 class I histocompatibility antigen, D-B alpha chain	HA11_MOUSE	P01899	0.027918	2.684921	1.424879
Protein canopy homolog 2	CNPY2_MOUSE	Q9QXT0	0.000789	2.682453	1.423553
Cathelicidin antimicrobial peptide	CAMP_MOUSE	P51437	0.007919	2.667416	1.415443
Proteasome activator complex subunit 2	PSME2_MOUSE	P97372	0.005792	2.655506	1.408987
Prolargin	PRELP_MOUSE	Q9JK53	0.009458	2.64374	1.40258
Protein S100-A9	S10A9_MOUSE	P31725	0.002422	2.634305	1.397422
NPC intracellular cholesterol transporter 2	NPC2_MOUSE	Q9Z0J0	0.029353	2.615949	1.387334
Nucleophosmin	NPM_MOUSE	Q61937	0.022951	2.610909	1.384552
Alpha-1-acid glycoprotein 1	A1AG1_MOUSE	Q60590	0.008631	2.589415	1.372626
Complement component 1 Q subcomponent-binding protein, mitochondrial	C1QBP_MOUSE	O35658	0.007318	2.518929	1.33281
40S ribosomal protein S28	RS28_MOUSE	P62858	0.017581	2.507979	1.326525
Osteoclast-stimulating factor 1	OSTF1_MOUSE	Q62422	0.019663	2.50497	1.324793
Glutamine amidotransferase-like class 1 domain-containing protein 1	GALD1_MOUSE	Q8BFQ8	0.013322	2.488572	1.315318
Anamorsin	CPIN1_MOUSE	Q8WTY4	0.000562	2.47118	1.3052
Histone H2A.V	H2AV_MOUSE	Q3THW5	0.03043	2.395832	1.260527
Keratin, type II cytoskeletal 5	K2C5_MOUSE	Q922U2	0.030186	2.390688	1.257426

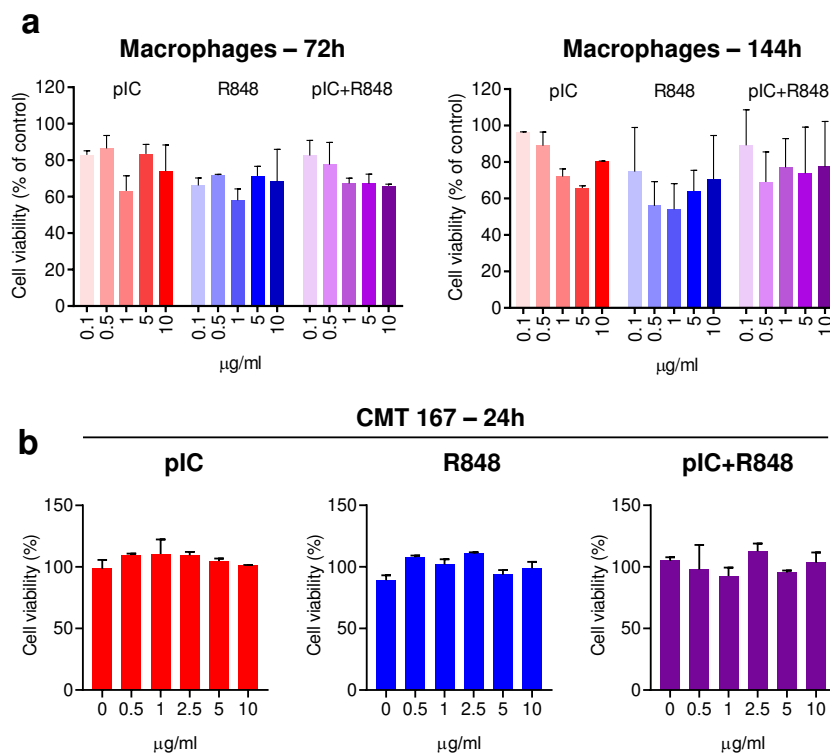
Hemopexin	HEMO_MOUSE	Q91X72	0.03061	2.386093	1.25465
Nucleosome assembly protein 1-like 1	NP1L1_MOUSE	P28656	0.000131	2.385584	1.254342
60S acidic ribosomal protein P2	RLA2_MOUSE	P99027	0.006066	2.377981	1.249737
Nuclease-sensitive element-binding protein 1	YBOX1_MOUSE	P62960	0.003197	2.251179	1.170681
Proteasome activator complex subunit 1	PSME1_MOUSE	P97371	0.003108	2.246398	1.167613
Nuclear migration protein nudC	NUDC_MOUSE	O35685	0.001598	2.216785	1.148469
Importin subunit alpha-1	IMA1_MOUSE	P52293	0.013745	2.206371	1.141675
Superoxide dismutase [Cu-Zn]	SODC_MOUSE	P08228	0.00948	2.194042	1.133591
Actin-related protein 2/3 complex subunit 3	ARPC3_MOUSE	Q9JM76	0.011305	2.184241	1.127132
Prosaposin	SAP_MOUSE	Q61207	0.036501	2.176941	1.122302
Tropomyosin alpha-4 chain	TPM4_MOUSE	Q6IRU2	0.023455	2.176285	1.121868
Cathepsin S	CATS_MOUSE	O70370	0.043281	2.172302	1.119224
RNA binding motif protein, X-linked-like-1	RMX1L_MOUSE	Q91VM5	0.001684	2.171622	1.118773
Galectin-3-binding protein	LG3BP_MOUSE	Q07797	0.013595	2.159094	1.110426
Leukotriene A-4 hydrolase	LKHA4_MOUSE	P24527	0.021819	2.151439	1.105302
Acidic leucine-rich nuclear phosphoprotein 32 family member E	AN32E_MOUSE	P97822	0.005278	2.144605	1.100712
Ubiquitin-conjugating enzyme E2 L3	UB2L3_MOUSE	P68037	0.00377	2.1316	1.091937
Receptor expression-enhancing protein 5	REEP5_MOUSE	Q60870	0.016304	2.129456	1.090485
Programmed cell death protein 5	PDCD5_MOUSE	P56812	0.028031	2.109901	1.077175
Small nuclear ribonucleoprotein Sm D2	SMD2_MOUSE	P62317	0.003308	2.094972	1.066931
DnaJ homolog subfamily C member 8	DNJC8_MOUSE	Q6NZB0	0.012186	2.091372	1.064449
Dipeptidyl peptidase 1	CATC_MOUSE	P97821	0.026786	2.072054	1.051062
Apolipoprotein E	APOE_MOUSE	P08226	0.027833	1.966694	0.975773
Proteasome subunit beta type-10	PSB10_MOUSE	O35955	0.000389	1.948096	0.962064
Apoptosis inhibitor 5	API5_MOUSE	O35841	0.024266	1.938637	0.955043
Tropomyosin alpha-3 chain	TPM3_MOUSE	P21107	0.018775	1.921747	0.942418
N-acetylglucosamine-6-sulfatase	GNS_MOUSE	Q8BFR4	0.013639	1.89016	0.918508
U1 small nuclear ribonucleoprotein A	SNRPA_MOUSE	Q62189	0.020782	1.875887	0.907573
Nucleolar RNA helicase 2	DDX21_MOUSE	Q9JIK5	0.013623	1.854313	0.890884
Collagen alpha-1(I) chain	CO1A1_MOUSE	P11087	0.045549	1.849683	0.887278
Transforming growth factor-beta-induced protein ig-h3	BGH3_MOUSE	P82198	0.017169	1.845052	0.883661
U2 small nuclear ribonucleoprotein A'	RU2A_MOUSE	P57784	0.005144	1.832036	0.873448
Lumican	LUM_MOUSE	P51885	0.011477	1.82844	0.870613
Guanylate-binding protein 2	GBP2_MOUSE	Q9Z0E6	0.033171	1.817772	0.862171
Leucine-rich repeat-containing protein 59	LRC59_MOUSE	Q922Q8	0.004851	1.779278	0.831292
Far upstream element-binding protein 1	FUBP1_MOUSE	Q91WJ8	0.006606	1.774477	0.827394
Acid ceramidase	ASAH1_MOUSE	Q9WV54	0.03543	1.77339	0.82651
Ras GTPase-activating protein-binding protein 1	G3BP1_MOUSE	P97855	0.04528	1.748435	0.806064
Calumenin	CALU_MOUSE	O35887	0.015917	1.726612	0.787944
rRNA 2'-O-methyltransferase fibrillar	FBRL_MOUSE	P35550	0.041236	1.721726	0.783855
RNA-binding protein EWS	EWS_MOUSE	Q61545	0.023194	1.706665	0.77118
Tryptophan--tRNA ligase, cytoplasmic	SYWC_MOUSE	P32921	0.018088	1.699466	0.765081
Transcription intermediary factor 1-beta	TIF1B_MOUSE	Q62318	0.027087	1.690199	0.757193
Eukaryotic translation initiation factor 3 subunit J-B	EI3JB_MOUSE	Q66J56	0.018771	1.679098	0.747686
Thioredoxin	THIO_MOUSE	P10639	0.012732	1.672173	0.741724
Nucleobindin-1	NUCB1_MOUSE	Q02819	0.020634	1.657199	0.728747
60S acidic ribosomal protein P1	RLA1_MOUSE	P47955	0.001853	1.654715	0.726583
Fibronectin	FINC_MOUSE	P11276	0.02132	1.631826	0.706487
Dynactin subunit 2	DCTN2_MOUSE	Q99KJ8	0.019084	1.631743	0.706414
Heterogeneous nuclear ribonucleoprotein K	HNRPK_MOUSE	P61979	0.00284	1.612236	0.689063
Cytochrome c, somatic	CYC_MOUSE	P62897	0.022466	1.60958	0.686685
Transgelin-2	TAGL2_MOUSE	Q9WVA4	0.030998	1.608983	0.686149
40S ribosomal protein S21	RS21_MOUSE	Q9CQR2	0.049559	1.606055	0.683521
Splicing factor U2AF 65 kDa subunit	U2AF2_MOUSE	P26369	0.003307	1.599522	0.67764
Protein NDRG1	NDRG1_MOUSE	Q62433	0.041428	1.574425	0.654825
Acylamino-acid-releasing enzyme	APEH_MOUSE	Q8R146	0.020654	1.56329	0.644586
26S proteasome non-ATPase regulatory subunit 7	PSMD7_MOUSE	P26516	0.016838	1.556534	0.638337

Protein disulfide-isomerase A3	PDIA3_MOUSE	P27773	0.043526	1.526871	0.610578
40S ribosomal protein S19	RS19_MOUSE	Q9CZX8	0.046784	1.514576	0.598914
Pro-cathepsin H	CATH_MOUSE	P49935	0.029448	1.499388	0.584374
Tumor protein D52	TPD52_MOUSE	Q62393	0.01001	1.498682	0.583694
Elongation factor 1-beta	EF1B_MOUSE	O70251	0.025011	1.498187	0.583218
Tubulin beta-5 chain	TBB5_MOUSE	P99024	0.03858	1.445894	0.531962
Protein S100-A4	S10A4_MOUSE	P07091	0.000992	1.421797	0.507715
Serine/arginine-rich splicing factor 2	SRSF2_MOUSE	Q62093	0.013223	1.418617	0.504485
Far upstream element-binding protein 2	FUBP2_MOUSE	Q3U0V1	0.022634	1.286285	0.363211
Acidic leucine-rich nuclear phosphoprotein 32 family member A	AN32A_MOUSE	O35381	0.012963	1.233492	0.302748

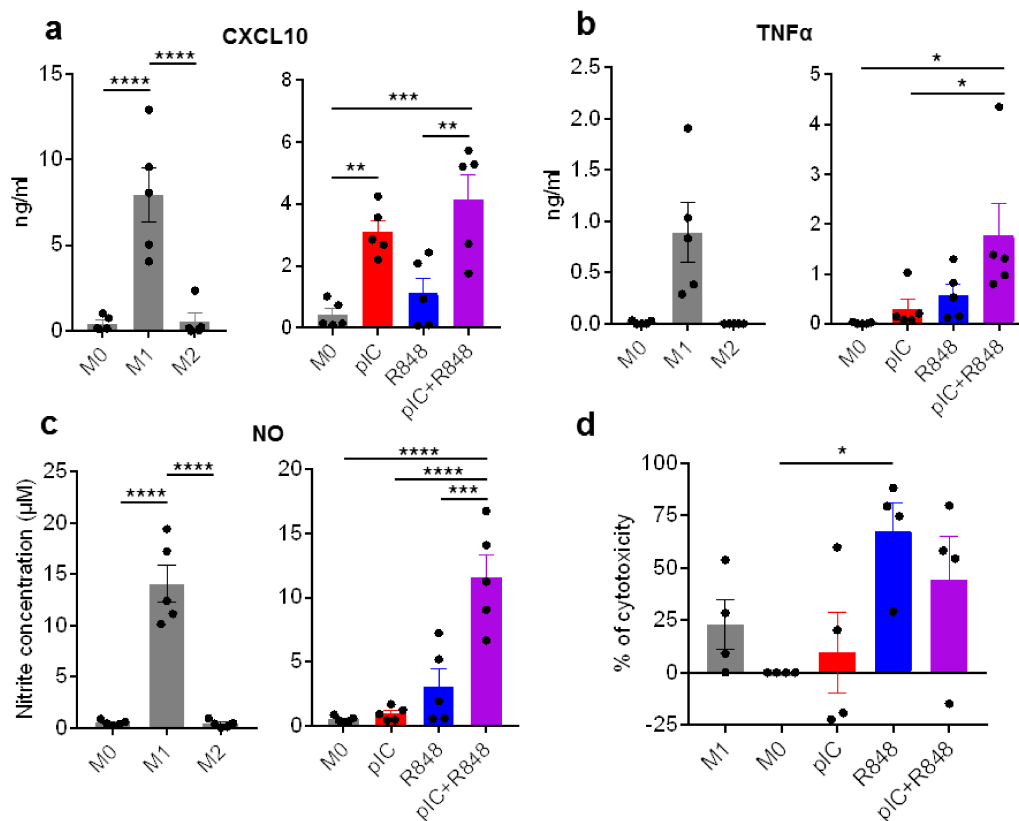
**Supplementary Table 8.** List of the down-regulated proteins in poly(I:C)+R848 treated tumors. FC, Fold change.

Down-regulated					
Protein	UniProt ID	UniProt accession	p-value	FC	Log 2 (FC)
Proteasome subunit beta type-5	PSB5_MOUSE	O55234	0.010934	0.27413588	-1.86704
Endophilin-B2	SHLB2_MOUSE	Q8R3V5	0.034988	0.344444925	-1.53765
Clusterin	CLUS_MOUSE	Q06890	0.0107	0.372689943	-1.42395
Glutathione S-transferase A4	GSTA4_MOUSE	P24472	0.038814	0.374923416	-1.41533
Latexin	LXN_MOUSE	P70202	0.011818	0.437030068	-1.1942
Eukaryotic translation initiation factor 3 subunit B	EIF3B_MOUSE	Q8JZQ9	0.026744	0.452935616	-1.14262
GTP-binding protein SAR1a	SAR1A_MOUSE	P36536	0.021724	0.465821112	-1.10215
Synaptic vesicle membrane protein VAT-1 homolog	VAT1_MOUSE	Q62465	0.021411	0.517886354	-0.94929
Serine hydroxymethyltransferase, mitochondrial	GLYM_MOUSE	Q9CZN7	0.00429	0.521725866	-0.93864
Receptor of activated protein C kinase 1	RACK1_MOUSE	P68040	0.034166	0.53882722	-0.89211
Pyruvate kinase PKM	KPYM_MOUSE	P52480	0.037207	0.545258131	-0.87499
Serpin B6	SPB6_MOUSE	Q60854	0.031656	0.568080208	-0.81583
U6 snRNA-associated Sm-like protein LSM3	LSM3_MOUSE	P62311	0.032094	0.575596616	-0.79687
Cystatin-B	CYTB_MOUSE	Q62426	0.027081	0.596730078	-0.74485
Fascin	FSCN1_MOUSE	Q61553	0.006595	0.602440911	-0.73111
Peroxiredoxin-1	PRDX1_MOUSE	P35700	0.032045	0.61244558	-0.70735
Adenosylhomocysteinase	SAHH_MOUSE	P50247	0.024563	0.613972563	-0.70375
L-lactate dehydrogenase A chain	LDHA_MOUSE	P06151	0.033025	0.638400728	-0.64747
40S ribosomal protein S23	RS23_MOUSE	P62267	0.0126	0.650476837	-0.62043
Rho GDP-dissociation inhibitor 1	GDIR1_MOUSE	Q99PT1	0.01772	0.657149344	-0.60571
UTP--glucose-1-phosphate uridylyltransferase	UGPA_MOUSE	Q91ZJ5	0.018093	0.664523742	-0.58961
4-trimethylaminobutyraldehyde dehydrogenase	AL9A1_MOUSE	Q9JLJ2	0.018487	0.66485955	-0.58888
40S ribosomal protein S3	RS3_MOUSE	P62908	0.023169	0.665478412	-0.58754
Elongation factor 2	EF2_MOUSE	P58252	0.00058	0.673322333	-0.57063
Bifunctional glutamate/proline--tRNA ligase	SYEP_MOUSE	Q8CGC7	0.023933	0.676107519	-0.56468
Isocitrate dehydrogenase [NADP], mitochondrial	IDHP_MOUSE	P54071	0.023137	0.69185014	-0.53147
Heat shock protein HSP 90-alpha	HS90A_MOUSE	P07901	0.039732	0.697124865	-0.52051
Inositol monophosphatase 1	IMPA1_MOUSE	O55023	0.035862	0.702724484	-0.50897
Fatty acid-binding protein, epidermal	FABP5_MOUSE	Q05816	0.015142	0.713853283	-0.4863
60S ribosomal protein L6	RL6_MOUSE	P47911	0.011992	0.723128491	-0.46768
D-3-phosphoglycerate dehydrogenase	SERA_MOUSE	Q61753	0.03453	0.726419541	-0.46113
60S ribosomal protein L11	RL11_MOUSE	Q9CXW4	0.002984	0.738353441	-0.43762
Eukaryotic translation initiation factor 2 subunit 1	IF2A_MOUSE	Q6ZWX6	0.01606	0.740392567	-0.43364
60S ribosomal protein L14	RL14_MOUSE	Q9CR57	0.015354	0.741438123	-0.4316
C-1-tetrahydrofolate synthase, cytoplasmic	C1TC_MOUSE	Q922D8	0.042916	0.741737805	-0.43102
Aldehyde reductase	ALDR_MOUSE	P45376	0.000337	0.745492421	-0.42373

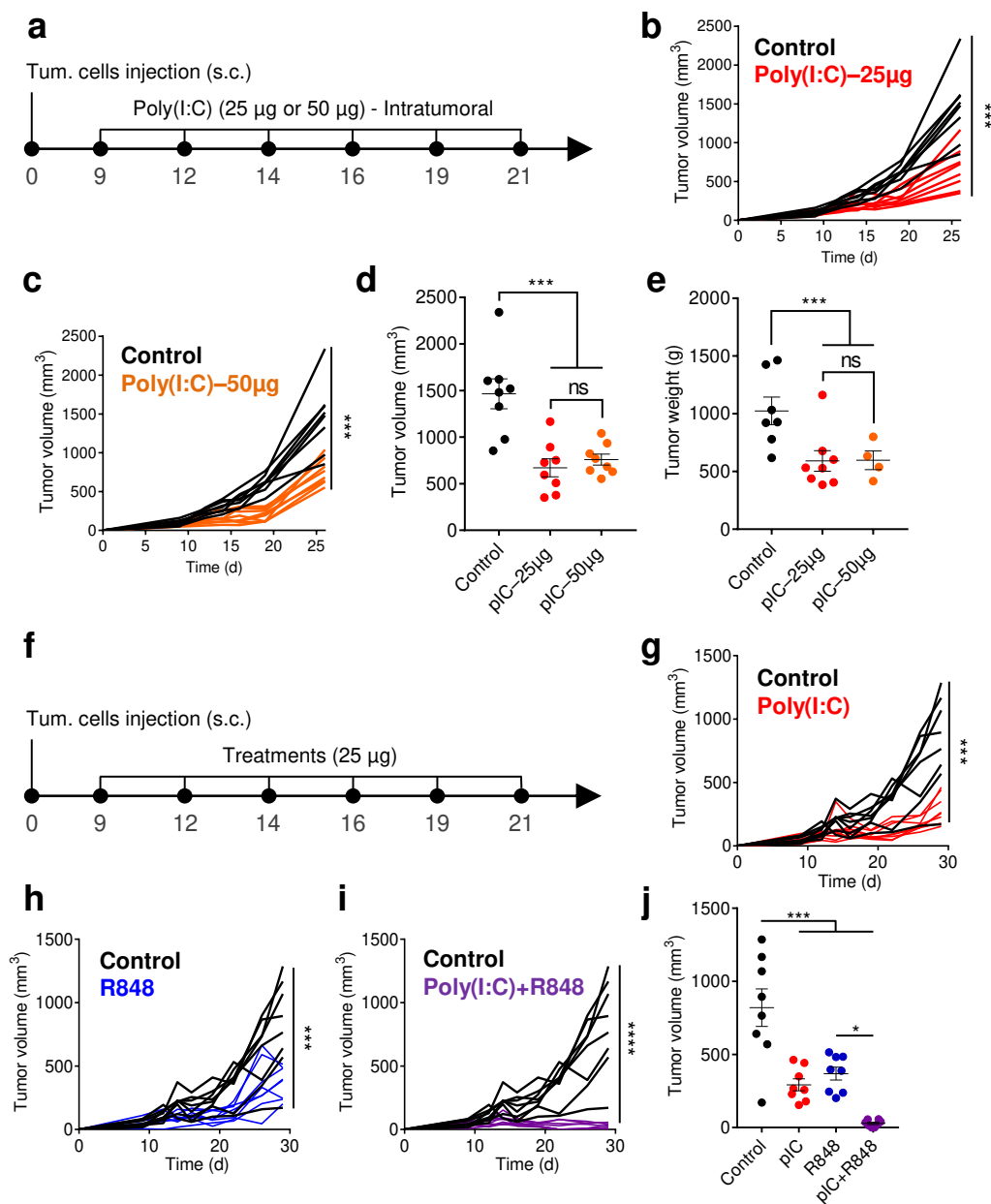
Cullin-associated NEDD8-dissociated protein 1	CAND1_MOUSE	Q6ZQ38	0.011313	0.748169437	-0.41856
Phosphoglycerate kinase 1	PGK1_MOUSE	P09411	0.046259	0.750602447	-0.41388
Heat shock protein HSP 90-beta	HS90B_MOUSE	P11499	0.027074	0.750977846	-0.41316
6-phosphogluconate dehydrogenase, decarboxylating	6PGD_MOUSE	Q9DCD0	0.00156	0.753605028	-0.40812
T-complex protein 1 subunit theta	TCPQ_MOUSE	P42932	0.023617	0.755901509	-0.40373
60S ribosomal protein L27	RL27_MOUSE	P61358	0.016738	0.758046368	-0.39964
Elongation factor 1-gamma	EF1G_MOUSE	Q9D8N0	0.037801	0.769735444	-0.37757
40S ribosomal protein S9	RS9_MOUSE	Q6ZWN5	0.025805	0.771736999	-0.37382
Clathrin heavy chain 1	CLH1_MOUSE	Q68FD5	0.018433	0.777335065	-0.36339
Bifunctional purine biosynthesis protein PURH	PUR9_MOUSE	Q9CWJ9	0.036711	0.785273148	-0.34873
Dihydropyrimidinase-related protein 2	DPYL2_MOUSE	O08553	0.030983	0.785989593	-0.34742
Ubiquitin carboxyl-terminal hydrolase 14	UBP14_MOUSE	Q9JMA1	0.005999	0.787665353	-0.34435
Isocitrate dehydrogenase [NADP] cytoplasmic	IDHC_MOUSE	O88844	0.048243	0.798599903	-0.32446
Polyadenylate-binding protein 1	PABP1_MOUSE	P29341	0.027583	0.810031027	-0.30395
60S ribosomal protein L18	RL18_MOUSE	P35980	0.013615	0.855088592	-0.22585
Actin-related protein 2/3 complex subunit 1B	ARC1B_MOUSE	Q9WV32	0.00622	0.866661129	-0.20646



**Supplementary Figure 1. Toxicological evaluation *in vitro* of poly(I:C) and R848, alone or combined, towards CMT167 cells or primary human monocyte derived macrophages exposed at longer times.** (a) Cell viability (Alamar Blue) of M0 macrophages exposed 72 h or 144 h to the drugs. M0 macrophages were isolated from peripheral blood mononuclear cells (PBMCs) stimulated with 25 ng/mL of rhM-CSF and cultured *in vitro* for 6 days (N=2). (b) Cell viability (Alamar Blue) of CMT167 cells exposed 24 h to the drugs (N=3). Values represent mean  $\pm$  s.e.m. Statistical comparison was performed using a one-way ANOVA test. No statistically significant differences were found for any group of treatment. pIC, poly(I:C); R848, resiquimod.

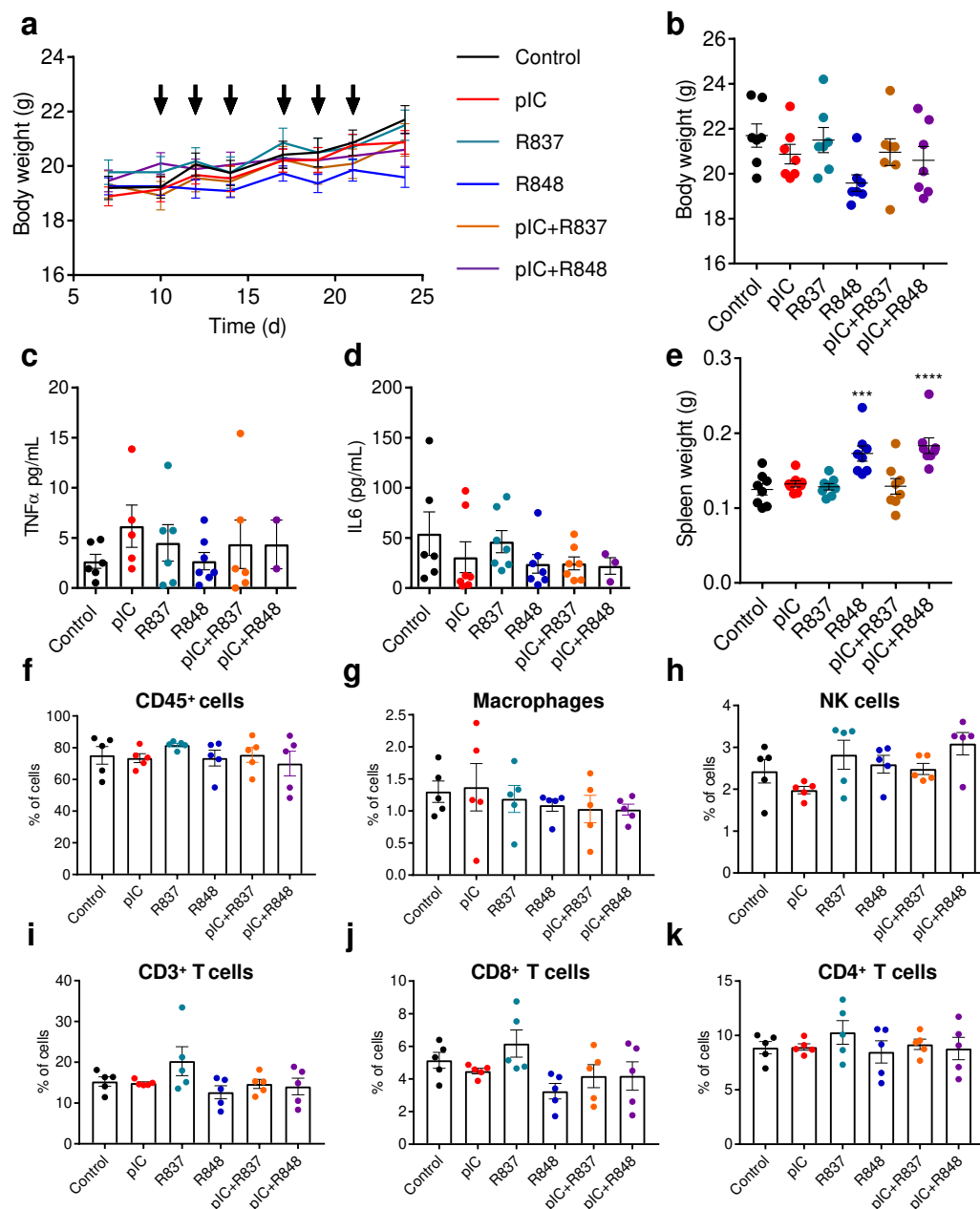


**Supplementary Figure 2. Immunomodulatory evaluation *in vitro* of poly(I:C) and R848, alone or combined, using primary murine macrophages.** Control macrophages were *in vitro* differentiated from murine bone-marrow derived macrophages (BMDMs) stimulated with 25 ng/mL of rmM-CSF for 5 days, and then polarized with 100 ng/mL of LPS and 50 ng/mL of IFN $\gamma$  (M1), 20 ng/mL of IL-4 (M2) or medium (M0) for 24 h. Each dot corresponds to distinct murine macrophages. ELISA evaluation of (a) CXCL10 and (b) TNF- $\alpha$  and (c) NO secretion by murine BMDMs exposed 24 h to the TLR agonists. (d) Cytotoxic activity of TLR-treated-BMDMs towards murine CMT167 cancer cells. BMDMs were treated for 24 h with TLR agonists, co-cultured for 48 h with cancer cells and analyzed by FACS, as represented in Fig. 1e (original manuscript). Bars represent mean  $\pm$  s.e.m. Statistical comparison was performed using a one-way ANOVA followed by a Tukey's multiple comparison test. Statistically significant differences are represented as \*( $p < 0.05$ ), \*\*( $p < 0.01$ ), \*\*\*( $p < 0.001$ ) and \*\*\*\*( $p < 0.0001$ ). pIC, poly(I:C); R848, resiquimod.



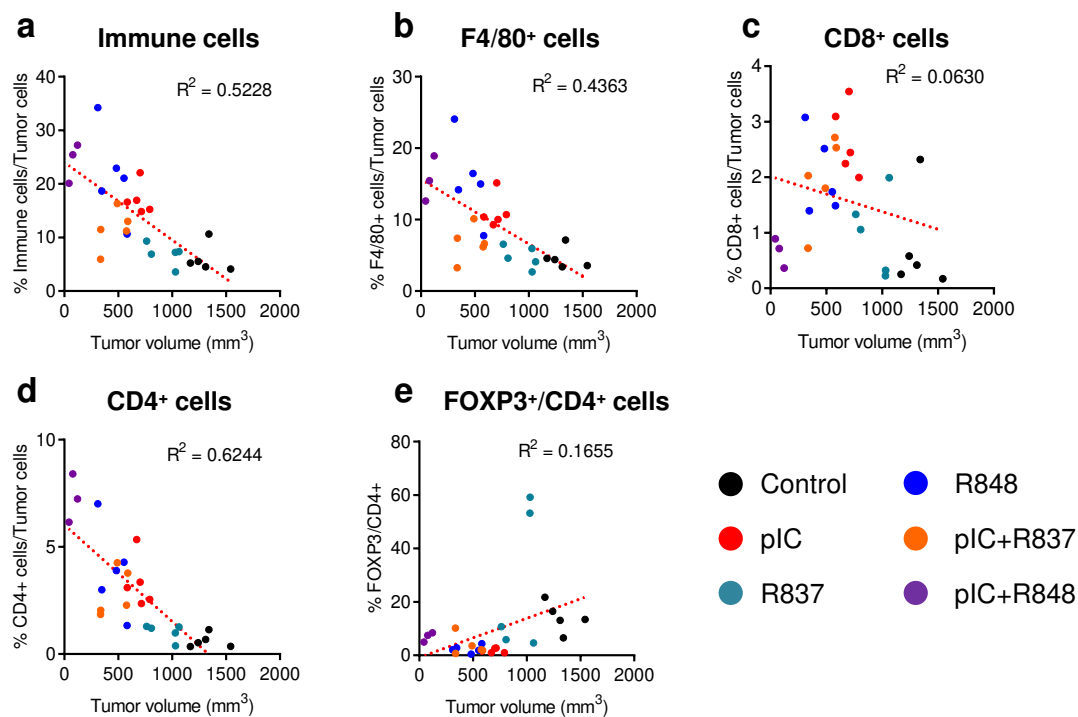
**Supplementary Figure 3. Antitumoral efficacy of intratumoral injections of poly(I:C) and R848, alone or combined, in the immunocompetent lung cancer murine model CMT167. (a-e)** Comparison of the antitumoral efficacy of two different doses of poly(I:C) applied intratumorally in the immunocompetent lung cancer murine model CMT167. **(a)** Schematic representation of the experimental protocol. **(b-e)** Evolution of tumor growth of mice treated with **(b)** 6x25  $\mu$ g of poly(I:C) and **(c)** 6x50  $\mu$ g of poly(I:C). **(d)** Comparison of tumor volume at sacrifice. **(e)** Comparison of tumor weight at sacrifice. **(f-j)** Antitumoral

efficacy of intratumoral injections of poly(I:C) and R848, alone or combined, in the immunocompetent lung cancer murine model CMT167. (f) Schematic representation of the experimental protocol. CMT167 cells were injected subcutaneously in the flank. From day 9 to day 21, mice received intratumoral delivery of TLR agonists (25 µg) as monotherapy or in combination. Control mice received only saline. (g–j) Evolution of tumor growth of mice treated with (g) poly(I:C), (h) R848 and (i) combination of Poly(I:C)+R848. (j) Comparison of tumor volume at sacrifice. Bars represent mean ± s.e.m ; N=8 per group. Statistical comparison was performed using a one-way ANOVA followed by a Tuckey's multiple comparison test. Statistically significant differences are represented as \*\*\*( $p < 0.001$ ) and \*\*\*\*( $p < 0.0001$ ) vs control; ns, not significant. pIC, poly(I:C); R848, resiquimod.

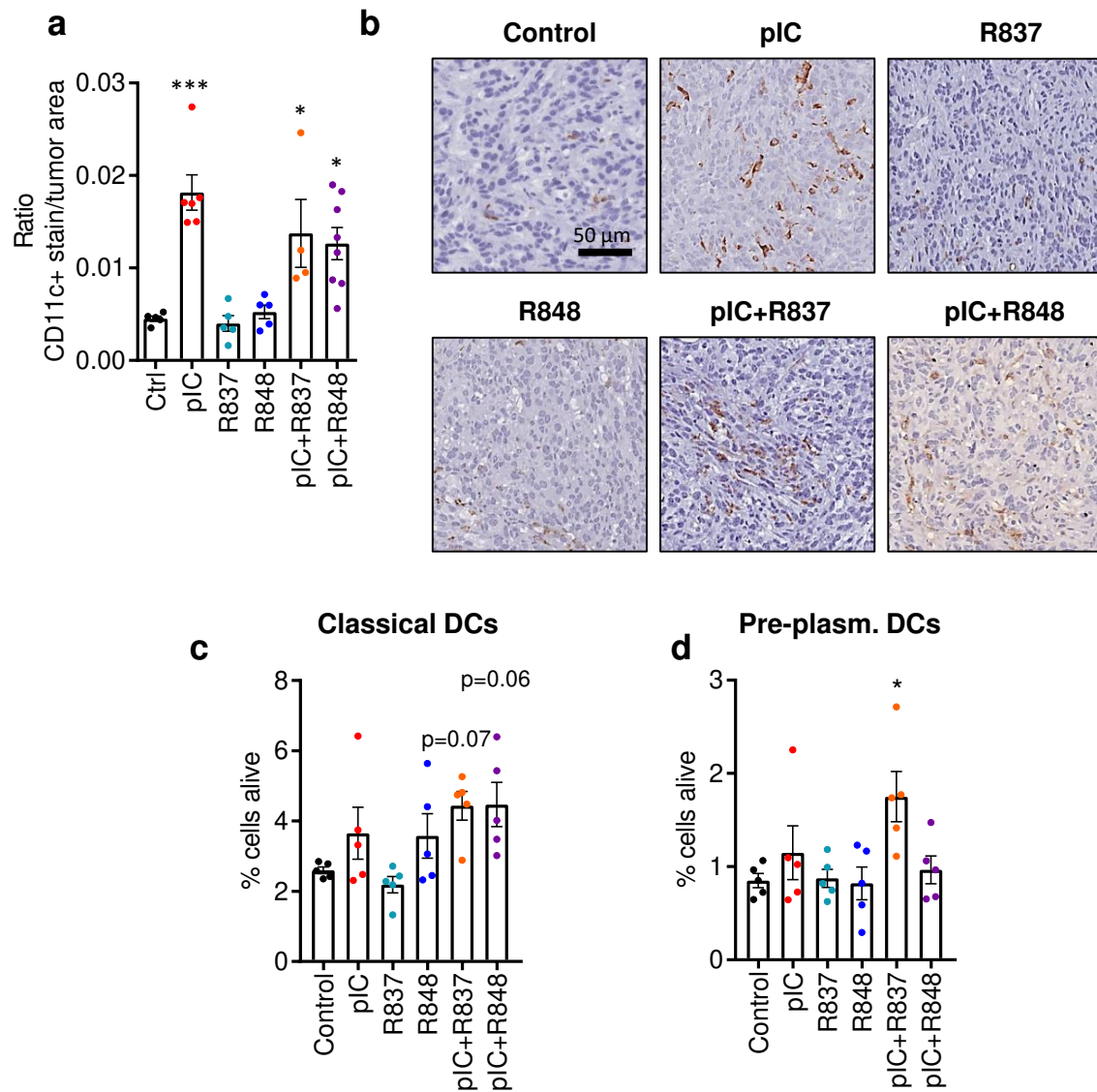


**Supplementary Figure 4. Lack of toxicity of intratumoral administration of TLR agonists alone or in combination.** Mice bearing CMT167 tumors were treated intratumorally with 6 injections of TLRs agonists (total of 150  $\mu$ g/mouse) alone or in combination. **(a)** Weight curves of tumor-bearing mice treated with 6 doses of TLRs agonists (arrows). N=8 per group. **(b)** Weight of individual mice, represented by points, at day 24. **(c-d)** Quantification of the circulation levels of **(c)** TNF- $\alpha$  and **(d)** IL-6 in the blood at day 24. **(e)** Weight of spleens at day 24. The spleen tissue was analyzed with flow cytometry for the proportion of **(f)** leukocytes (CD45<sup>+</sup>) in living cells, **(g)** macrophages (CD45<sup>+</sup>, CD11b<sup>+</sup>, F4/80<sup>+</sup>), **(h)** NK cells (CD45<sup>+</sup>, NK1.1<sup>+</sup>), **(i)** T lymphocytes (CD45<sup>+</sup>, CD3<sup>+</sup>), **(j)** CD8<sup>+</sup> T lymphocytes and **(k)**

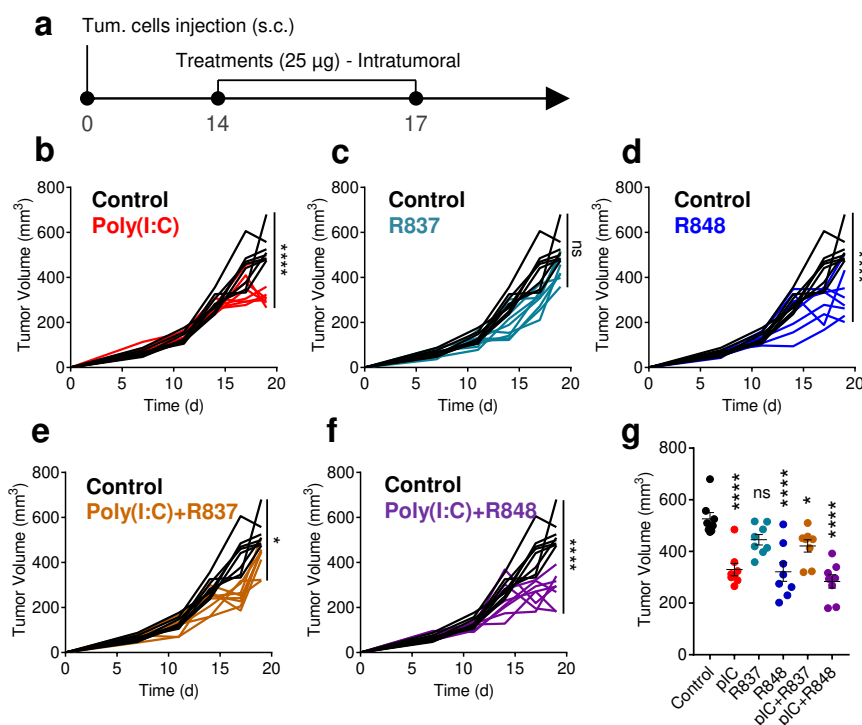
CD4<sup>+</sup> T lymphocytes. Bars represent mean  $\pm$  s.e.m. Statistical comparison was performed using a one-way ANOVA followed by a Dunnett's multiple comparison test. Statistically significant differences are represented as \*\*\*( $p < 0.001$ ) and \*\*\*\*( $p < 0.0001$ ) vs control. pIC, poly(I:C); R837, imiquimod; R848, resiquimod.



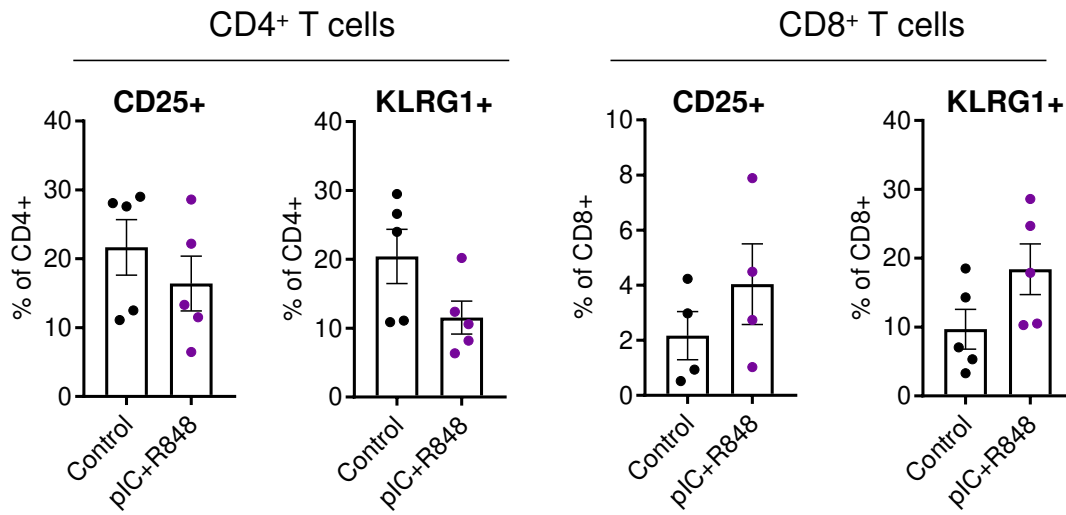
**Supplementary Figure 5. Multiplexed immunofluorescence analysis of immune infiltration in CMT167 tumors treated with TLR-agonist monotherapies or combinations.** Correlation between tumor volume and immunofluorescence analysis quantification of (a) total immune cells, (b) macrophages (F4/80+), (c) CD8+ T cells, (d) CD4+ T cells and (e) FOXP3+/CD4+ T cells in treated tumors. Each dot corresponds to a single animal. pIC, poly(I:C); R837, imiquimod; R848, resiquimod.



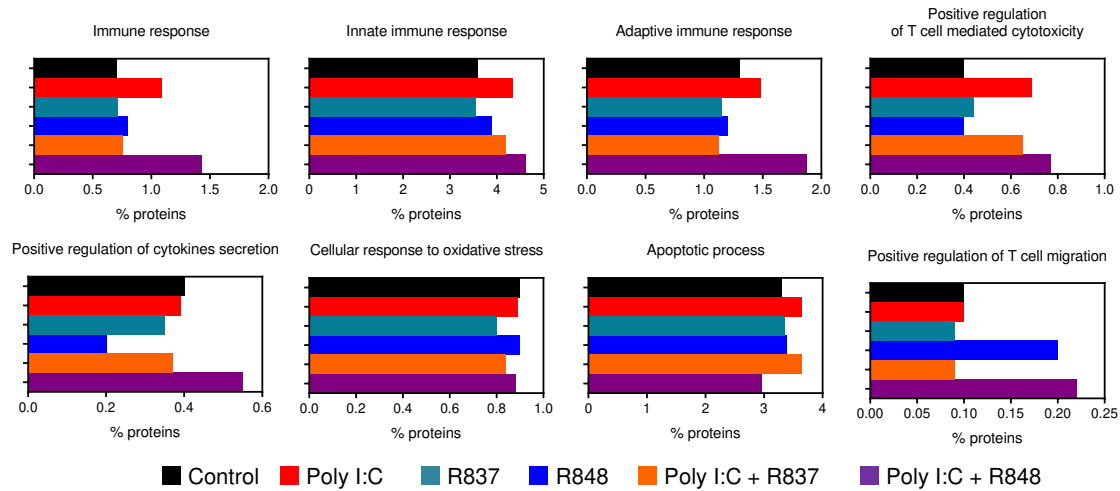
**Supplementary Figure 6. Analysis of dendritic cells infiltration in CMT167 tumors treated with TLR-agonist monotherapies or combinations.** (a) Immunohistochemistry quantification for CD11c in CMT167 tumors i.t. treated with 6 injections of TLR agonists and (b) representative pictures from tumors stained for CD11c. In CMT167 tumors i.t. treated with 2 injections of TLR agonists, intratumoral proportion of (c) classical dendritic cells (CD11b<sup>+</sup>, CD11c<sup>int</sup>) and (d) pre-plasmocytoid dendritic cells (CD11b<sup>-</sup>, CD11c<sup>+</sup>) were analysed with flow cytometry. Bars represent mean ± s.e.m. Statistical comparison was performed using a one-way ANOVA followed by a Dunnett's multiple comparison test. Statistically significant differences are represented as \*(p<0.05) and \*\*\*(p<0.001) vs control. pIC, poly(I:C); R837, imiquimod; R848, resiquimod.



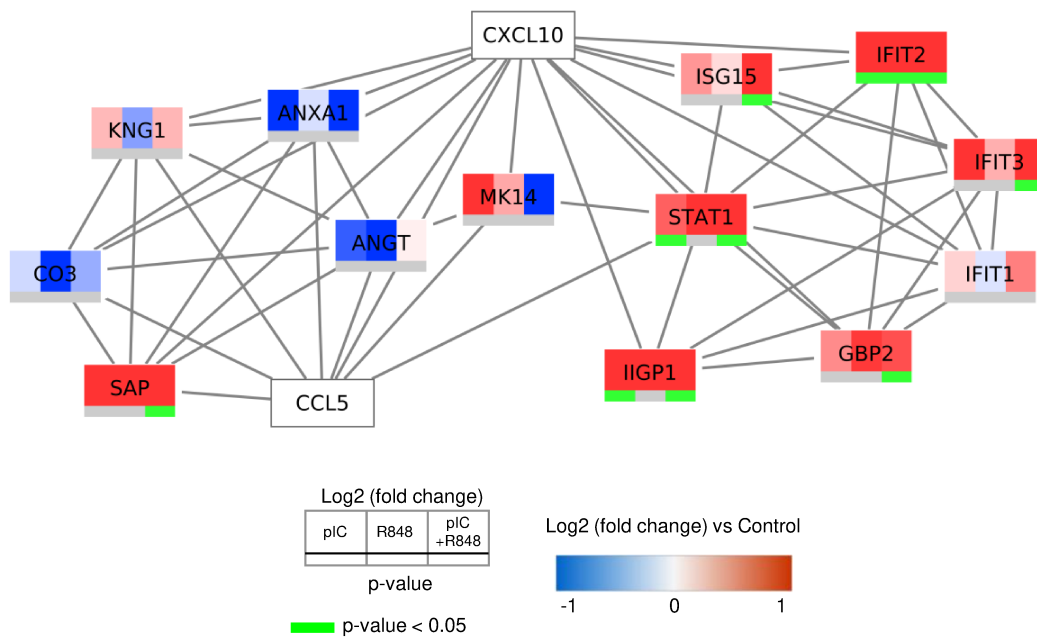
**Supplementary Figure 7. Antitumoral efficacy of poly(I:C), R837 and R848, alone or combined, applied intratumorally (2 injections) in the immunocompetent lung cancer murine model CMT167. (a)** Schematic representation of the experimental protocol. **(b–f)** Evolution of tumor growth of mice treated with **(b)** poly(I:C), **(c)** R837, **(d)** R848, **(e)** combination of poly(I:C) and R837 and **(f)** combination of poly(I:C) and R848. **(g)** Comparison of the tumor volume at sacrifice. Bars represent mean  $\pm$  s.e.m ; N=8 per group. Statistical comparison was performed using a one-way ANOVA followed by a Tukey's multiple comparison test. Statistically significant differences are represented as \*( $p < 0.05$ ) and \*\*\*\*( $p < 0.001$ ) vs control; ns, not significant. pIC, poly(I:C); R837, imiquimod; R848, resiquimod.



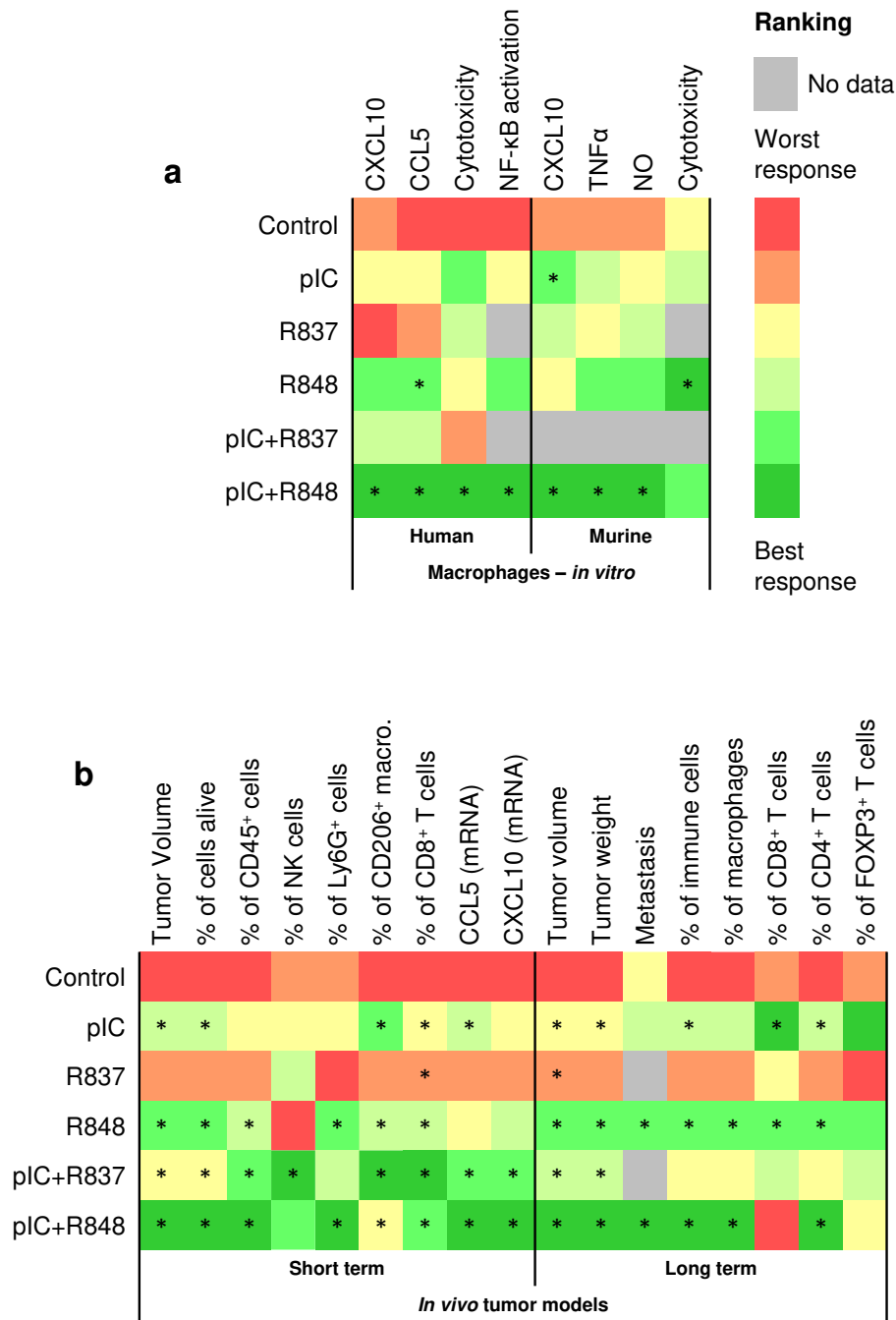
**Supplementary Figure 8. FACS analysis of activation markers in CD4<sup>+</sup> and CD8<sup>+</sup> T cells.** CMT167 tumors i.t. treated with 2 injections of poly (I:C)+R848 were analyzed with flow cytometry for the proportion of CD25<sup>+</sup> and KLRG1<sup>+</sup> cells in CD4<sup>+</sup> and CD8<sup>+</sup> T cells. N=5 per group. Bars represent mean ± s.e.m. pIC, poly(I:C); R848, resiquimod.



**Supplementary Figure 9. Qualitative proteomic analysis reveals the molecular mediators of antitumor immune responses triggered in TLR treated tumors, N=3 mice per group of treatment. FunRich functional analysis results of proteins detected for each biological process. Qualitative comparison between groups. pIC, Poly I:C; R837, imiquimod; R848, resiquimod.**



**Supplementary Figure 10. Protein-protein interaction network analysis, with a high-confidence score (> 0.7) for CXCL10 and CCL5 in tumors treated with poly(I:C) (left), R848 (center) and poly(I:C)+R848 (right). Red and blue indicate increased and decreased log<sub>2</sub> (fold change) compared to control, respectively. Green color indicates significance (p<0.05).**



**Supplementary Figure 11. The poly(I:C)+R848 combination induces a superior antitumoral response, versus single treatments or poly(I:C)+R837, through STAT1 activation and macrophage reprogramming. Comparison of the (a) *in vitro*, (b) short-term and long-term *in vivo* responses to the**

TLR-treatments observed in this study. \* indicates treatments that induced a response statistically different *versus* the control ( $p < 0.05$ ).